El-Fakharany, M.; Company Rossi, R.; Jódar Sánchez, LA. (2016). Solving partial integro-differential option pricing problems for a wide class of infinite activity Lévy processes. Journal of Computational and Applied Mathematics. 296:739-752. doi:10.1016/j.cam.2015.10.027.

Solving partial integro-differential option pricing problems for a wide class of infinite activity Lévy processes

M. Fakharany, R. Company[1], L. Jódar

Instituto de Matemática Multidisciplinar, Universitat Politècnica de València, Camino de Vera s/n, 46022 Valencia, Spain

Abstract

In this paper, numerical analysis of finite difference schemes for partial integro-differential models related to European and American option pricing problems under a wide class of Lévy models is studied. Apart from computational and accuracy issues, qualitative properties such as positivity are treated. Consistency of the proposed numerical scheme and stability in the Von Neumann sense are included. Gauss-Laguerre quadrature formula is used for the discretization of the integral part. Numerical examples illustrating the potential advantages of the presented results are included.

Keywords: Numerical analysis, partial integro-differential equation, option pricing, Gauss-Laguerre quadrature, positivity.

1. Introduction

Since a long time ago empirical observations of the market show the evidence that the price of the underlying asset does not behave like a Brownian motion with a drift and a constant volatility. This fact motivates the emergence of alternative models to the pioneering Black-Scholes model [1]. Alternative models are stochastic volatility [2], deterministic volatility [3], jump diffusion [4, 5, 6, 7]

Email addresses: fakharany@aucegypt.edu (M. Fakharany), rcompany@imm.upv.es (R. Company), ljodar@imm.upv.es (L. Jódar)

[1]corresponding author

and infinite activity Lévy models.

One of the most relevant and versatile Lévy models is the one proposed by Carr *et. al.* the so called CGMY [8], that belongs to the family of KoBoL models [9]. Apart from these models, other Lévy processes such as Meixner [10, 11], Hyperbolic and Generalized Hyperbolic (**GH**) are used to obtain better estimation for the stock returns [12]. The Meixner process was introduced in 1998, it is used when the environment is changing stochastically over the time showing a reliable valuation for some indices such as Nikkei 225 [10].

The generalized hyperbolic distribution was introduced by Barndorff-Nielsen [13] and used to generate Lévy process to capture the real stock price movements of the intraday scale. It is exactly a pure discontinuous behavior of its paths what can be observed [12, 14]. Beside that the hyperbolic process is obtained as a special case from the (**GH**) process, it is implemented in various stock markets such as the blue chips of the German market, the DAX and also US stock market showing effective estimation for their returns [15].

However, following [12] the calibration of market option prices shows that depending on datasets, the matching between the actual price and the its corresponding estimated value varies form model to another consequently, we can not say which is the perfect one.

In this paper we study the option pricing partial integro-differential equation (PIDE) unified model for several Lévy measures $\nu(y)$, given by [16, Chap. 12]

$$\frac{\partial \mathcal{C}}{\partial \tau}(S,\tau) = \frac{\sigma^2}{2}S^2\frac{\partial^2 \mathcal{C}}{\partial S^2}(S,\tau) + (r-q)S\frac{\partial \mathcal{C}}{\partial S}(S,\tau) - r\mathcal{C}(S,\tau)$$

$$+\int_{-\infty}^{+\infty}\nu(y)\big[\mathcal{C}(Se^y,\tau)-\mathcal{C}(S,\tau)-S(e^y-1)\frac{\partial \mathcal{C}}{\partial S}(S,\tau)\big]dy,\ S\in(0,\infty),\ \tau\in(0,T], \tag{1}$$

$$\mathcal{C}(S,0) = f(S) = (S-E)^+, \qquad S\in(0,\infty), \tag{2}$$

$$\mathcal{C}(0,\tau) = 0; \lim_{S\to\infty}\mathcal{C}(S,\tau) = Se^{-q\tau} - Ee^{-r\tau}, \tag{3}$$

Model	The corresponding Lévy measure
KoBoL	$\nu(y) = \frac{C_- e^{-\mathcal{G}\|y\|}}{\|y\|^{1+Y}}\mathbf{1}_{y<0} + \frac{C_+ e^{-\mathcal{M}\|y\|}}{\|y\|^{1+Y}}\mathbf{1}_{y>0}$
Meixner	$\nu(y) = \frac{Ae^{-ay}}{y\sinh(by)}$
GH process	$\nu(y) = \frac{e^{\beta y}}{\|y\|}\left(\int_0^\infty \frac{e^{-\sqrt{2\zeta+\alpha^2}\|y\|}}{\pi^2\zeta\left(J^2_{\|\lambda\|}(\delta\sqrt{2\zeta}) + Y^2_{\|\lambda\|}(\delta\sqrt{2\zeta})\right)}d\zeta + \max(0,\lambda)e^{-\alpha\|y\|}\right)$

Table 1: The forms of $\nu(y)$

where $\mathcal{C}$ is the value of a contingent claim, S is the underlying asset and $\tau = T-t$ is the time to the maturity. The Lévy measures $\nu(y)$ are given in Table 1.

Note that the Hyperbolic process is obtained from the **GH** process when $\beta = 0$ and $\lambda = -1$.

To the best of our knowledge, the numerical solution and analysis of Meixner and **GH** models have not been treated. The KoBoL model and in particular the CGMY, see Table 1 with parameter $C_- = C_+$, has been widely studied because its versatile and includes the finite and infinite activity cases as well as the finite and infinite variation, obtained by changing the value of Yor parameter $Y < 2$. A fairly complete revision of the methods used to solve the CGMY model can be found in [17, 18, 19, 20].

In this paper we focus on the numerical analysis of the unified model (1)-(3) for the European case, by proposing a consistent, explicit and conditionally positive and stable finite difference scheme while the integral part is approximated using Gauss-Laguerre quadrature formula. We also include the computation of the linear complementarity problem (LCP) for the American option case using both the projected successive over relaxation method (PSOR) and the multigrid method (MG). The discretization for the differential operator is done using the three-level approximation, while the integral part is discretized as the same as in the European case. So, the integral part of the PIDE operator for the American and European cases is discretized using the Gauss-Laguerre quadra-

ture. Although the three-level method is widely used and it is argued that the approximation error is of order two, however such method has two unsuitable properties, in fact as the method needs the first time step that must be obtained using another method (usually by implicit Euler method), in practice the accuracy is reduced. Also, as it is shown in Example 1 for European option, the three-level method does not guarantee the positiveness.

With respect to previous relevant papers in the field, we should mention the potential advantage of our approach. Apart from the more general unified treatment of a wide class of Lévy models, we do not truncate the integral part for its approximation using Gauss-Laguerre quadrature that reduces the computational cost using a few amount of nodes to approximate the integral and improves the accuracy due to the advantages of Gauss-Laguerre quadrature. An additional positive fact of this approach is that it allows to give error information of the integral approximation as it is shown in Example 4.

The paper is organized as follows. In Section 2, the kernel singularity of the integral part of the PIDE is replaced by adding a diffusion term following the approach developed in [17, 18]. Then the reaction and convection terms of the differential part are removed by using suitable transformation as in [20]. Finally in Section 2, the numerical scheme construction is included. Section 3 deals with the numerical analysis of the explicit proposed numerical scheme, including conditional positivity and stability in the Von Neumann sense, as well as the consistency. Section 4 is addressed to the study of the American option case, the LCP is solved using the PSOR and MG including the Gauss-Laguerre quadrature discretization for the integral part and the three-level for the differential part. Section 5 includes numerical examples to discuss and validate the results. The Barrier option case is particularly interesting for its application to credit risk problems [21]. In Example 7, we have included the valuation of Barrier option with our approach.

For the sake of clarity, useful integral formula is included. The exponential

integral $E_s(\eta)$ is defined by [22, Chap. 5, p. 228]

$$E_s(\eta) = \int_1^\infty t^{-s} e^{-\eta t} dt. \tag{4}$$

2. Scheme construction for European options

Let us begin this section by transforming the PIDE (1) into a simpler one. Since the kernel of the integral in (1) presents a singularity at $y = 0$, a useful technique is to split the real line, for an arbitrary small parameter $\varepsilon > 0$, into two regions $\Omega_1 = [-\varepsilon, \varepsilon]$ and $\Omega_2 = \mathbb{R}\backslash\Omega_1$, the complementary set of Ω_1 in the real line. The integral on Ω_1 is replaced by a suitable coefficient in the diffusion term of the differential part of (1) obtained by Taylor expansion of $V(Se^y, \tau)$ about S, see [17, 18, 19, 20]. This coefficient depending on ε is a convergent integral and takes the form

$$\breve{\sigma}^2(\varepsilon) = \int_{-\varepsilon}^{\varepsilon} \nu(y)(e^y - 1)^2 dy = \varepsilon \int_{-1}^{1} \nu(\varepsilon\phi)(e^{\varepsilon\phi} - 1)^2 d\phi. \tag{5}$$

The resulting approximating PDE is given by

$$\frac{\partial \mathcal{C}}{\partial \tau} = \frac{\hat{\sigma}^2}{2} S^2 \frac{\partial^2 \mathcal{C}}{\partial S^2} + (r - q - \gamma(\varepsilon)) S \frac{\partial \mathcal{C}}{\partial S} - (r + \lambda(\varepsilon))\mathcal{C}$$

$$+ \int_{\Omega_2} \nu(y)\mathcal{C}(Se^y, \tau) dy, \tag{6}$$

where

$$\hat{\sigma}^2 = \sigma^2 + \breve{\sigma}^2(\varepsilon),\ \gamma(\varepsilon) = \int_{\Omega_2} \nu(y)(e^y - 1) dy,\ \lambda(\varepsilon) = \int_{\Omega_2} \nu(y) dy. \tag{7}$$

The convergent integrals (5) and (7) are evaluated using Gauss quadrature approximation. In order to obtain an approximation for $\breve{\sigma}^2(\varepsilon)$, the Legendre-Gauss quadrature approximation is used, so the weighting function $w(\phi) = 1$ such that

$$\breve{\sigma}^2(\varepsilon) \approx \varepsilon \sum_{m=1}^{M} \omega_m \nu(\varepsilon\phi_m)(e^{\varepsilon\phi_m} - 1)^2, \tag{8}$$

where ϕ_m are the roots of the Legendre polynomial $P_M(\phi)$ of degree M and ω_m is calculated based on [22, Eq. (25.4.29) p. 887]. Here M is chosen to be

an even number so that zero is not a root of P_M. The improper integrals $\lambda(\varepsilon)$ and $\gamma(\varepsilon)$ are approximated using the shifted Laguerre-Gauss quadrature [23, p. 226]. Note that under change of variables $\eta = -y - \varepsilon$ for $y < 0$ and $\eta = y - \varepsilon$ for $y > 0$ then $\lambda(\varepsilon)$ and $\gamma(\varepsilon)$ have the following forms

$$\lambda(\varepsilon) = \int_0^\infty (\nu(-\eta - \varepsilon) + \nu(\eta + \varepsilon))\, d\eta \tag{9}$$

and

$$\gamma(\varepsilon) = \int_0^\infty \left[\nu(-\eta - \varepsilon)(e^{-(\eta+\varepsilon)} - 1) + \nu(\eta + \varepsilon)(e^{\eta+\varepsilon} - 1)\right] d\eta. \tag{10}$$

From (9), (10) and since the weighting function is $w(\eta) = e^{-\eta}$, then we have

$$\lambda(\varepsilon) \approx \sum_{m=1}^{M} \varpi_m F(\eta_m, \varepsilon),\ \gamma(\varepsilon) \approx \sum_{m=1}^{M} \varpi_m \mathcal{F}(\eta_m, \varepsilon), \tag{11}$$

where

$$F(\eta, \varepsilon) = e^{\eta}(\nu(-\eta - \varepsilon) + \nu(\eta + \varepsilon))$$
$$\mathcal{F}(\eta, \varepsilon) = e^{\eta}\left(\nu(-\eta - \varepsilon)(e^{-(\eta+\varepsilon)} - 1) + \nu(\eta + \varepsilon)(e^{\eta+\varepsilon} - 1)\right).$$

Here η_m are the roots of the Laguerre polynomial $L_M(\eta)$ of degree M and the weighting function ϖ_m is given in [22, Eq. (25.4.45) p. 890].

Coming back to (6) in order to eliminate the convection and reaction terms, using the transformation defined by

$$x = \exp[(r - q - \gamma(\varepsilon))\tau]S,\ V(x, \tau) = \exp[(r + \lambda(\varepsilon))\tau]\mathcal{C}(S, \tau), \tag{12}$$

one gets

$$\frac{\partial V}{\partial \tau} = \frac{\hat{\sigma}^2}{2} x^2 \frac{\partial^2 V}{\partial x^2} + \int_{\Omega_2} \nu(y) V(xe^y, \tau) dy, \quad x \in (0, \infty), \quad \tau \in (0, T], \tag{13}$$

with the initial and boundary conditions

$$V(x, 0) = f(x) = (x - E)^+ \tag{14}$$

$$V(0, \tau) = 0; \quad \lim_{x \to \infty} V(x, \tau) = e^{\lambda(\varepsilon)\tau}(xe^{\gamma(\varepsilon)\tau} - E). \tag{15}$$

Next, for the sake of convenience in the numerical treatment we rewrite the integral part of (13) as follows

$$\int_{\Omega_2} \nu(y)V(xe^y,\tau)dy = \int_{-\infty}^{\infty} \hat{\nu}(y)V(xe^y,\tau)dy, \tag{16}$$

where

$$\hat{\nu}(y) = \begin{cases} \nu(y), & y \in \Omega_2 \\ 0, & y \in \Omega_1 \end{cases}. \tag{17}$$

After that, in order to match the interval of the integration with the spatial domain of the problem, we use the following substitution $\phi = xe^y$ into (16), obtaining

$$\int_{\Omega_2} \nu(y)V(xe^y,\tau)dy = \int_0^{\infty} \hat{\nu}(\ln(\frac{\phi}{x}))V(\phi,\tau)\frac{d\phi}{\phi}. \tag{18}$$

Hence the PIDE for the European option under Lévy model, takes the following form

$$\frac{\partial V}{\partial \tau} = \frac{\hat{\sigma}^2}{2}x^2\frac{\partial^2 V}{\partial x^2} + \int_0^{\infty} \hat{\nu}(\ln(\frac{\phi}{x}))V(\phi,\tau)\frac{d\phi}{\phi}. \tag{19}$$

Now, we are in a good situation to construct an efficient explicit numerical scheme for the transformed problem (19) after choosing our numerical domain $[0, x_{\max}] \times [0, T]$ for large enough value of $x_{\max}$. Based on [24] the suggested value of $x_{\max}$ is about $3E$ or $4E$.

- For the time discretization, we take $\tau^n = nk$, $n = 0, 1, \ldots, N_\tau$ where $k = \frac{T}{N_\tau}$.
- The spatial variable x is discretized by $x_j = jh$, $j = 0, 1, 2, \ldots, N_x$, $h = \frac{x_{\max}}{N_x}$.

Since the Laguerre-Gauss quadrature will be used for approximating the integral part of (19), then we have the sequence of roots $\{\phi_m\}_{m=1}^M$ of the Laguerre polynomial $L_M(\phi)$. The suitable value for M is selected such that $E < \phi_M < x_{\max}$.

By using explicit forward approximation for the time derivative of V and the central difference approximation for second spatial derivative, one gets

$$\frac{\partial V}{\partial \tau}(x_j,\tau^n) \approx \frac{V_j^{n+1} - V_j^n}{k}, \quad \frac{\partial^2 V}{\partial x^2}(x_j,\tau^n) \approx \frac{V_{j+1}^n - 2V_j^n + V_{j-1}^n}{h^2}. \tag{20}$$

In order to approximate the integral part of (19) matching the discretization of the integral and differential parts, taking into account that zeroes of Laguerre polynomial do not need to be nodes of the mesh, we use linear Lagrange interpolation polynomial. For any m, $1 \leq m \leq M$, let us denote by ℓ_m the last integer such that the mesh point $x_{\ell_m} < \phi_m$. The approximating value $V^n(\phi_m)$ is given by

$$V^n(\phi_m) = \tilde{a}_{\ell_m} V^n_{\ell_m} + \hat{a}_{\ell_m} V^n_{\ell_m+1}, \tag{21}$$

where the interpolation coefficients are

$$\tilde{a}_{\ell_m} = \frac{(x_{\ell_m+1} - \phi_m)}{h}; \quad \hat{a}_{\ell_m} = \frac{(\phi_m - x_{\ell_m})}{h}. \tag{22}$$

Note that the linear interpolation approximation (21) has an error of order $\mathcal{O}(h^2)$ that coincide with the associated error of the central approximation of the spatial derivative (20). Hence the discretization for the integral part is given by

$$I^n_j = \sum_{m=1}^{M} \hat{\nu}(\ln \frac{\phi_m}{x_j}) \frac{e^{\phi_m}}{\phi_m} \varpi_m \left(\tilde{a}_{\ell_m} V^n_{\ell_m} + \hat{a}_{\ell_m} V^n_{\ell_m+1} \right). \tag{23}$$

Summarizing, from (20)-(23), the discretization of (19) with (14) and (15) takes the form

$$V^{n+1}_j = \alpha_j (V^n_{j+1} + V^n_{j-1}) + \beta_j V^n_j + k \sum_{m=1}^{M} \hat{\nu}(\ln \frac{\phi_m}{x_j}) \frac{e^{\phi_m}}{\phi_m} \varpi_m \left(\tilde{a}_{\ell_m} V^n_{\ell_m} + \hat{a}_{\ell_m} V^n_{\ell_m+1} \right), \tag{24}$$

$1 \leq j \leq N_x - 1, \quad 0 \leq n \leq N_\tau - 1$, where

$$\alpha_j = \frac{k}{2h^2} \hat{\sigma}^2 x_j^2, \qquad \beta_j = 1 - 2\alpha_j, \tag{25}$$

satisfying

$$V^0_j = (x_j - E)^+, \tag{26}$$

and

$$V^n_0 = 0, \qquad V^n_{N_x} = e^{\lambda(\varepsilon)\tau^n} (x_{\max} e^{\gamma(\varepsilon)\tau^n} - E). \tag{27}$$

3. Numerical Analysis for European Options

Dealing with option prices, positive values of the numerical solution is a necessary requirement. In this section the positivity, stability as well as the consistency of the scheme (24)-(27) are studied. Note that the coefficients of scheme (24) are nonnegative under the condition

$$\frac{k}{h^2} \leq \frac{1}{\hat{\sigma}^2 x_{\max}^2}. \tag{28}$$

Thus from nonnegative initial and boundary values (26) and (27), the following result is immediate

Theorem 1. *The numerical solution* $\{V_j^n\}$ *of the scheme* (24)-(27) *is nonnegative under the condition* (28).

There are many approaches in the literature to study the stability for a finite difference scheme and many concepts of stability. Here we study the stability using the well known Von Neumann approach [25, 26]. Von Neumann analysis for linear parabolic PDEs with variable coefficients is treated in [27, 28][25, p. 59] and for PIDEs by [29]. Let us rewrite the numerical solution V_j^n

$$V_j^n = \xi^n e^{i\theta jh}, \tag{29}$$

where ξ^n is the amplitude at time level n, i is the imaginary unit and θ is the phase angle. According to [26, p. 68] the unconditional stability of scheme (24) is guaranteed if the amplification factor $G = \frac{\xi^{n+1}}{\xi^n}$ satisfies

$$|G| \leq 1 + Kk = 1 + \mathcal{O}(k), \tag{30}$$

where the positive number K is independent of h, k and θ.
When (30) is verified for those values of h and k satisfying a specific condition, then the stability of the scheme is said to be conditional.
By substituting into (24), one gets

$$G = 1 - a(k, h, \theta) + kz(j, h, \theta), \tag{31}$$

where

$$a(k,h,\theta) = 4\alpha_j \sin^2\left(\frac{\theta h}{2}\right), \tag{32}$$

$$z(j,h,\theta) = \sum_{m=1}^{M} A_{j,m} e^{i(\ell_m - j)\theta h} \left(\tilde{a}_{\ell_m} + \hat{a}_{\ell_m} e^{i\theta h}\right), \tag{33}$$

$$A_{j,m} = \hat{\nu}\left(\ln\frac{\phi_m}{x_j}\right)\varpi_m \frac{e^{\phi_m}}{\phi_m}. \tag{34}$$

Note that under the positivity condition (28) we have

$$\alpha_j = \frac{k}{2h^2}\hat{\sigma}^2 x_j^2 \leq \frac{1}{2}; \quad 4\alpha_j \sin^2\left(\frac{\theta h}{2}\right) \leq 2. \tag{35}$$

Thus

$$|1 - a(k,h,\theta)| \leq 1, \tag{36}$$

for h and k satisfying (28).

Under condition (28) from (31) and (36) one gets

$$\begin{aligned} |G|^2 &= (1 - a(k,h,\theta))^2 + 2k(1 - a(k,h,\theta))Re(z) + k^2|z|^2 \\ &\leq 1 + 2|z|k + |z|^2 k^2. \end{aligned} \tag{37}$$

Consequently, the stability will be guaranteed if $|z|$ is bounded.

Now we are interested in obtaining a common bound for $|z|$ for all the infinite activity Lévy models considered in Table 1.

from (22), $\tilde{a}_{\ell_m} + \hat{a}_{\ell_m} = 1$, and from (33) one gets

$$|z| \leq \sum_{m=1}^{M} A_{j,m}(\tilde{a}_{\ell_m} + \hat{a}_{\ell_m}) = \sum_{m=1}^{M} A_{j,m}. \tag{38}$$

Note that from (9) and (34), $\sum_{m=1}^{M} A_m^j$ is the Gauss-Laguerre quadrature approximation for $\lambda(\varepsilon)$, then for an arbitrarily small $\rho > 0$ and large enough value of M one gets

$$\sum_{m=1}^{M} A_{j,m} \leq \rho + \int_{\varepsilon}^{\infty} (\nu(-y) + \nu(y))dy. \tag{39}$$

It is easy to check from Table 1 that for all Lévy measures,

$$\nu(-y) + \nu(y) < \mathfrak{G}(y), \quad y \in (\varepsilon, \infty), \tag{40}$$

where

$$\mathfrak{G}(y) = 2\hat{C}\frac{e^{-\hat{M}y}}{y^{1+\hat{Y}}}, \tag{41}$$

and

$$\hat{C} = \begin{cases} \max(C_-, C_+), & \text{KoBoL} \\ \frac{2}{b}A, & \text{Meixner} \\ 2\max(|\lambda|, \tilde{C}_M), & \text{Generalized Hyperbolic,} \end{cases} \tag{42}$$

such that

$$\tilde{C}_M = \sum_{m=1}^{M} \frac{\varpi_m e^{\phi_m}}{\pi^2 \phi_m (J^2_{|\lambda|}(\delta\sqrt{(}2\phi_m)) + Y^2_{|\lambda|}(\delta\sqrt{(}2\phi_m)))},$$

$$\hat{M} = \begin{cases} \min(\mathcal{G}, \mathcal{M}), & \text{KoBoL} \\ a, & \text{Meixner} \\ \alpha - |\beta|, & \text{Generalized Hyperbolic} \end{cases} \tag{43}$$

$$\hat{Y} = \begin{cases} Y, & \text{KoBoL} \\ 1, & \text{Meixner} \\ 0, & \text{Generalized Hyperbolic} \end{cases} . \tag{44}$$

From (40) and (41), it follows that

$$\int_{\varepsilon}^{\infty} (\nu(-y) + \nu(y))dy < \int_{\varepsilon}^{\infty} \mathfrak{G}(y)dy = 2\hat{C}\varepsilon^{-\hat{Y}} E_{1+\hat{Y}}(\varepsilon\hat{M}), \tag{45}$$

where $E_s(\eta)$ is the exponential integral defined by (4).

Hence from (38), we have

$$|z| \leq \sum_{m=1}^{M} A_m^j \leq 2\hat{C}\varepsilon^{-\hat{Y}} E_{1+\hat{Y}}(\varepsilon\hat{M}). \tag{46}$$

Summarizing the following result has been established.

Theorem 2. *With previous notation, under the positivity condition* (28)*, the numerical scheme* (24) *for* (19) *is conditionally stable.*

Once the stability has been established, in order to guarantee the convergence of the numerical scheme for the linear PIDE problem it is sufficient to prove the consistency of the numerical scheme with the PIDE. According to its

definition [26, 30], a numerical scheme is consistent with a PIDE problem if the exact theoretical solution of the PIDE approximates well the difference scheme as the stepsizes discretization tend to zero.

Let us denote $v_j^n = V(x_j, \tau^n)$ as the value of the exact solution of (19). The local truncated error $T_j^n(V)$ at (x_j, τ^n) is defined by

$$T_j^n(V) = \left(\frac{v_j^{n+1} - v_j^n}{k} - \frac{\hat{\sigma}^2}{2}\frac{x_j^2}{h^2}(v_{j-1}^n - 2v_j^n + v_{j+1}^n) - \frac{\partial V}{\partial \tau}(x_j, \tau^n) + \frac{\hat{\sigma}^2}{2}x^2\frac{\partial^2 V}{\partial x^2}(x_j, \tau^n) \right)$$

$$- \left(\sum_{m=1}^{M} A_{j,m} \left(\tilde{a}_{\ell_m} v_{\ell_m}^n + \hat{a}_{\ell_m} v_{\ell_m+1}^n \right) - \int_0^\infty \hat{\nu}(\ln \frac{\phi}{x}) V(\phi, \tau) \frac{d\phi}{\phi} \right) \tag{47}$$

$$= L(V_j^n) - I(V_j^n), \tag{48}$$

where $L(V_j^n)$ and $I(V_j^n)$ denote the truncation errors for the differential and integral parts respectively. In order to prove the consistency, we must show that

$$T_j^n(V) \to 0, \text{ as } h \to 0, \ k \to 0. \tag{49}$$

Assuming that V is twice continuously partially differentiable with respect to τ and four times partially differentiable with respect to x, and using Taylor's expansion about (x_j, τ^n), it is easy to obtain

$$L(V_j^n) = \mathcal{O}(h^2) + \mathcal{O}(k), \tag{50}$$

see [20] for a detailed development of this expression. The local truncation error for the integral part is given by

$$|I(V_j^n)| = \left| \int_0^\infty \hat{\nu}(\ln(\frac{\phi}{x_j})) V(\phi, \tau^n) \frac{d\phi}{\phi} - \sum_{m=1}^{M} \hat{\nu}(\ln \frac{\phi_m}{x_j}) \varpi_m \frac{e^{\phi_m}}{\phi_m} V(\phi_m, \tau^n) \right| \tag{51}$$

$$= ((M!)^2) \hat{f}[\phi_1, \phi_1, \phi_2, \phi_2, \ldots, \phi_M, \phi_M, \hat{\xi}], \tag{52}$$

where $\hat{f}[\phi_1, \phi_1, \phi_2, \phi_2, \ldots, \phi_M, \phi_M, \hat{\xi}]$ denotes the divided difference for

$$\hat{f}(\phi) = \hat{\nu}(\ln(\frac{\phi}{x_j})) \frac{e^\phi}{\phi} V(\phi, \tau^n), \hat{\xi} > 0, \tag{53}$$

see [31, p. 397 Eq. (8.7.12)]. For smooth enough integrands the error takes the form

$$|I(V_j^n)| = \frac{(M!)^2}{2M!}\hat{f}^{(2M)}(\hat{\xi}). \tag{54}$$

Summarizing the scheme (24) is consistent with the PIDE (19) and the truncation error behaves

$$T_j^n = \mathcal{O}(h^2) + \mathcal{O}(k) + \epsilon(M), \tag{55}$$

where M is the number of the roots of Laguerre polynomial of degree M used in the numerical integration.

4. American options under Lévy models

The most used method for pricing an American option is the formulation of a LCP and then solving it using a numerical method, see [18, 32, 33]. Following this approach the LCP for American option under the Lévy measures in Table 1 and the transformation (12) takes the form

$$\mathcal{L}[V] \geq 0, \quad V \geq f(x), \quad \mathcal{L}[V](V - f(x)) = 0, \tag{56}$$

where

$$\mathcal{L}[V] = \frac{\partial V}{\partial \tau} - \mathcal{D}[V] - I(V), \tag{57}$$

and $f(x)$ is the payoff given by (14). The operators $\mathcal{D}[V]$ and $I(V)$ are given by

$$\mathcal{D}[V] = \frac{\hat{\sigma}^2}{2}x^2\frac{\partial^2 V}{\partial x^2}, \quad I(V) = \int_{\Omega_2} \nu(y)V(xe^y, \tau)dy. \tag{58}$$

Let us obtain the semi-discrete formulation of the problem (56). Using spatial central difference approximation for the second derivative and Laguerre Gauss quadrature for the integral part, one gets

$$\mathcal{D}[V] + I(V) \approx \hat{\alpha}_j(V_{j-1} - 2V_j + V_{j+1}) + \sum_{m=1}^{M} A_{j,m}\left(\tilde{a}_{\ell_m}V_{\ell_m} + \hat{a}_{\ell_m}V_{\ell_m+1}\right), \tag{59}$$

where $\hat{\alpha}_j = \frac{\hat{\sigma}^2 x_j^2}{2h^2}$; $\tilde{a}_{\ell_m}$, $\hat{a}_{\ell_m}$ and $A_{m,j}$ are given in (22) and (34) respectively. Let $\mathcal{A} \in \mathbb{R}^{(Nx-1)\times(Nx-1)}$ be the matrix representation of (59)

$$\mathcal{A} = -\hat{\mathcal{D}} - \mathcal{P}, \tag{60}$$

where the entries $d_{j\ell}$ of the tridiagonal matrix $\hat{\mathcal{D}}$ are given by

$$d_{j\ell} = \begin{cases} -2\hat{\alpha}_j, & \ell = j, \\ \hat{\alpha}_j, & \ell = j-1, j+1. \end{cases} \tag{61}$$

Let us introduce the sets

$$\hat{L}_1 = \{\ell_m\}_{m=1}^{M}, \quad \hat{L}_2 = \{\ell_m + 1\}_{m=1}^{M}, \quad \tilde{m} : \ell_m \to m. \tag{62}$$

The matrix $\mathcal{P}$ for the integral part is represented as

$$\mathcal{P} = \tilde{\mathcal{P}} + \hat{\mathcal{P}}, \tag{63}$$

where

$$\tilde{p}_{j\ell} = \begin{cases} A_{j,\tilde{m}(\ell)}\tilde{a}_\ell, & \ell \in \hat{L}_1, \\ 0, & \text{otherwise}, \end{cases}, \quad \hat{p}_{j\ell} = \begin{cases} A_{j,\tilde{m}(\ell)}\hat{a}_\ell, & \ell \in \hat{L}_2, \\ 0, & \text{otherwise}. \end{cases} \tag{64}$$

With the above notations the LCP (56) has the following semi-discrete form

$$\frac{\partial \mathbf{V}}{\partial \tau} + \mathcal{A}\mathbf{V} \geq \mathbf{b}(\tau); \quad \mathbf{V} \geq \mathbf{f}; \quad \left(\frac{\partial \mathbf{V}}{\partial \tau} + \mathcal{A}\mathbf{V} - \mathbf{b}(\tau)\right)^T (\mathbf{V} - \mathbf{f}) = 0, \tag{65}$$

where $\mathbf{V} = \mathbf{V}(\tau)$ is the vector solution satisfying $\mathbf{V}(0) = \mathbf{f}$ and $\mathbf{b} = \mathbf{b}(\tau)$ is the vector including the boundary conditions

$$\mathbf{V} = [V_1 \; V_2 \ldots V_{N_x - 1}], \quad \mathbf{b} = [V_0 \; 0 \; 0 \ldots 0 \; V_{N_x}(\tau)]. \tag{66}$$

Explicit time discretization is not suitable for LCP problems because of the computational cost. Also, the Crank-Nicolson approximation is convenient when the initial data and its derivative are continuous. As this is not our case we choose the three time levels which also known as the backward difference formula (BDF2) with accuracy of second order like Crank-Nicolson and better stability properties [32, 34]. Hence the corresponding LCP for (65) after time discretization is denoted by

$$LCP(\tilde{\mathcal{A}}, \mathbf{V}^{n+1}, \tilde{\mathbf{V}}^n, \mathbf{f}), \tag{67}$$

and given by

$$\tilde{\mathcal{A}}\mathbf{V}^{n+1} - \tilde{\mathbf{V}}^n \geq 0; \quad \mathbf{V}^{n+1} \geq \mathbf{f}; \quad (\tilde{\mathcal{A}}\mathbf{V}^{n+1} - \tilde{\mathbf{V}}^n)^T (\mathbf{V}^{n+1} - \mathbf{f}), \tag{68}$$

where

$$\tilde{\mathcal{A}} = \begin{cases} I + k\mathcal{A}, & n = 0, \\ I + \frac{2k}{3}\mathcal{A}, & n \geq 1, \end{cases} \tag{69}$$

and

$$\tilde{\mathbf{V}}^n = \begin{cases} \mathbf{V}^0 + k\mathbf{b}^0, & n = 0, \\ \frac{4}{3}\mathbf{V}^n - \frac{1}{3}\mathbf{V}^{n-1} + \frac{2k}{3}\mathbf{b}^{n+1}, & n \geq 1. \end{cases} \tag{70}$$

Note that the first level for the solution vector is obtained using the implicit Euler approximation. Also, the matrix $\tilde{\mathcal{A}}$ is of M-Matrix type.

The pioneering method PSOR introduced by Cryer [35] is commonly used to solve LCPs. The crux of this method is to execute successive over relaxed modifications for the solution vector components associated with a projection when any component be less than the payoff. The relaxation parameter $\omega \in (0, 2)$ plays a relevant role accelerating the rate of convergence and the optimal value for ω can be calculated by the expression [26]

$$\omega_{op} = \frac{2}{1 + \sqrt{1 - \rho^2(\mathbf{G})}}, \tag{71}$$

where $\mathbf{G} = \mathbf{D}^{-1}(\tilde{\mathcal{A}} - \mathbf{D})$ is the Jacobi iteration matrix, $\mathbf{D}$ is the diagonal of $\tilde{\mathcal{A}}$ and $\rho(\mathbf{G})$ is the spectral radius of $\mathbf{G}$.

When solving a LCP using PSOR, one has to address two challenges; firstly the selection of the initial guess, secondly its accuracy declines as the grid becomes finer [36]. The multigrid iterative method **MG**) has been shown as a reliable alternative to overcome the quoted difficulties [37, 38, 39]. The operator that transforms the problem from the coarser to the finer grid is called the linear interpolation (prolongation) operator and symbolized by I_{2h}^h, while the map for the inverse transformation is called the full weighting restriction operator and denoted by I_h^{2h}. Here, the matrix $\tilde{\mathcal{A}}^h$ denotes the matrix $\tilde{\mathcal{A}}$ on the finer grid and $\tilde{\mathcal{A}}^{2h}$ is the corresponding matrix on the coarse grid and obtained by [37]

$$\tilde{\mathcal{A}}^{2h} = I_h^{2h}\tilde{\mathcal{A}}^h I_{2h}^h. \tag{72}$$

Remark

The three time-level can be used for European option but it does not guarantee the positivity of the solution, see Example 1. The corresponding scheme is given by

$$(I + \frac{2k}{3}\mathcal{A})\mathbf{V}^{n+1} = \frac{4}{3}\mathbf{V}^{n} - \frac{1}{3}\mathbf{V}^{n-1} + \frac{2k}{3}\mathbf{b}^{n+1}, \quad n \geq 1, \tag{73}$$

and the first level solution is obtained by

$$(I + k\mathcal{A})\mathbf{V}^{1} = \mathbf{V}^{0} + k\mathbf{b}^{0}. \tag{74}$$

5. Numerical Examples

In this section five numerical examples are included to validate, compare and discuss the proposed results. From Example 1 to Example 4 are related to European option case; Example 1 deals with the positivity, Example 4 discuss the consistency and Examples 2 and 3 report about accuracy and computational cost. Finally Example 5 deals with the American option case. The numerical examples are done using Matlab on a Microprocessor 3.4 GHz Intel Core i7. Throughout the examples related to European options, we will refer as scheme 1 to explicit scheme (24)-(27) and scheme 2 as the three-level scheme (73)-(74). The objective of the first example is to exhibit the importance of the positivity condition (28) for the three studied Lévy models.

Example 1. Here, we have an European option with $E = 30$, $T = 0.5$, $r = 0.08$, $q = 0$, $\sigma = 0.2$, $x_{\min} = 0$, $x_{\max} = 90$, $M = 15$, $\varepsilon = 0.5$ and $N_x = 128$. The parameters for Lévy models are given in Table 2. Figure 1 displays the behavior of the option price $\mathcal{C}$ evaluated by the proposed explicit scheme (24)-(27) when the positivity condition (28) holds for $N_\tau = 25e3$ and when it is broken for $N_\tau = 1e3$ represented by the solid and dot curves respectively under several Lévy processes.

In spite of the computational performance of the three level method, from the qualitative point of view, it disregards some important issues as the positivity. With the same parameters, $N_x = 800$ and several values of N_τ Table 3 shows

Model	Parameters
CGMY	$C = 0.5$, $\mathcal{G} = 15$, $\mathcal{M} = 25$ and $Y = 1.2945$.
Meixner	$A = 0.5$, $a = -2.5$ and $b = 8$.
GH	$\alpha = 4$, $\beta = -3.2$, $\delta = 0.4775$ and $\lambda = 2$

Table 2: The parameters for Lévy models used in Example 1.

negative values of the option price under CGMY process valuated with (73)-(74).

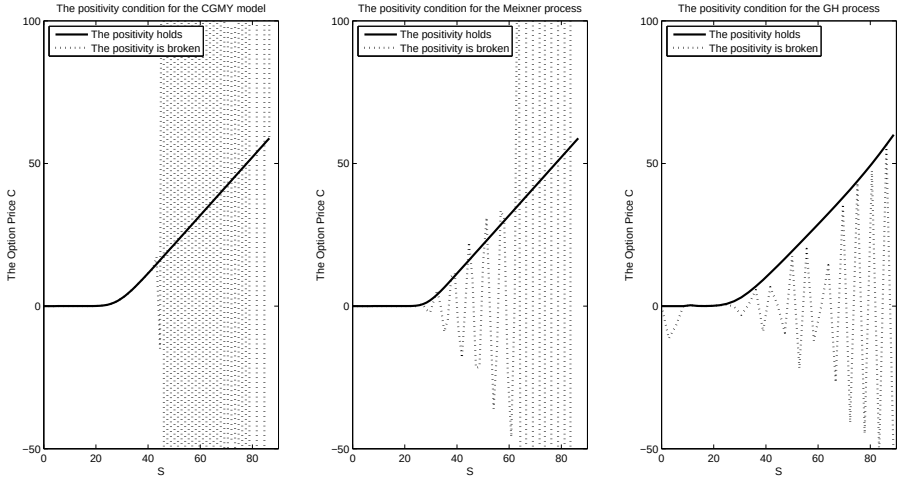

Fig. 1. About positivity condition of explicit scheme .

The aim of the next example is to show the variation of the error for the Variance Gamma **VG** model as the stepsizes h and k change. The **VG** is obtained from the CGMY model when $Y = 0$, the reference option values for $S = \{20, 30, 40, 50\}$ are obtained using the closed form solution given in [40].

Example 2. Consider an European option under the **VG** process with parameters $E = 30$, $T = 0.5$, $r = 0.1$, $q = 0$, $\sigma = 0.25$, $C_- = C_+ = 11.718$,

N_τ	S		
	8	10	12
20	-1.58e-2	-1.17e-2	-5.64e-3
40	-8.33e-3	-6.12e-3	-2.78e-3
80	-3.61e-3	-2.82e-3	-1.16e-3
160	-1.62e-3	-1.37e-3	-4.63e-4

Table 3: Computed negative values with the three-level method.

	S	20		30		40		50		CPU
	N_x	**AE**	α	**AE**	α	**AE**	α	**AE**	α	in sec
Scheme 1	32	8.909e-4	–	1.926e-3	–	3.742e-3	–	4.386e-3	–	1.84
	64	2.409e-4	1.89	5.335e-4	1.85	1.022e-3	1.87	1.181e-3	1.89	4.63
	128	6.363e-5	1.92	1.413e-4	1.92	2.710e-4	1.91	3.053e-4	1.95	10.85
	256	1.552e-5	2.04	3.698e-5	1.93	6.952e-5	1.96	7.603e-5	2.01	18.99
Scheme 2	32	1.091e-3	–	1.477e-3	–	1.713e-3	–	4.873e-4	–	0.64
	64	2.861e-4	1.93	3.956e-4	1.89	4.238e-4	2.01	1.297e-4	1.91	1.31
	128	7.386e-5	1.95	1.043e-4	1.95	1.090e-4	1.96	3.340e-5	1.93	3.60
	256	1.783e-5	2.05	2.470e-5	2.08	2.550e-5	2.09	8.067e-6	2.07	8.29

Table 4: Errors and convergence rates for the VG model for several values of N_x.

$\mathcal{G} = 15$ and $\mathcal{M} = 25$, $x_{\min} = 0$, $x_{\max} = 90$, $M = 15$, $\varepsilon = 0.35$. Table 4. reveals the variation of the absolute error (**AE**) as h changes as well as the spatial numerical convergence rate α and the CPU time while $N_\tau = 4.5e3$ for the explicit scheme 1 (24) and $N_\tau = 256$ for the three-level scheme 2 (73)-(74). The change of the error due to the variation of N_τ, its convergence rate β and the elapsed time are shown in Table 5 while $N_x = 128$.

The third example shows the variation of the root mean square relative error

	S	20		30		40		50		CPU
	N_τ	**AE**	β	**AE**	β	**AE**	β	**AE**	β	in sec
Scheme 1	1.2e3	2.161e-4	–	4.790e-4	–	9.243e-4	–	1.151e-3	–	4.06
	2.4e3	1.154e-4	0.91	2.552e-4	0.89	4.883e-4	0.92	6.049e-4	0.93	7.28
	4.8e3	5.883e-5	0.97	1.304e-4	0.94	2.519e-4	0.95	3.072e-4	0.98	12.65
	9.6e3	2.916e-5	1.02	6.462e-5	0.96	1.288e-4	0.97	1.489e-5	1.04	20.37
Scheme 2	32	9.751e-4	–	1.661e-3	–	1.455e-3	–	4.807e-4	–	0.83
	64	5.046e-4	0.95	8.395e-4	0.98	7.325e-4	0.99	2.467e-4	0.96	1.46
	128	2.144e-4	1.23	3.215e-4	1.38	3.048e-4	1.26	9.843e-5	1.32	2.78
	256	7.386e-5	1.54	1.043e-4	1.62	1.090e-4	1.48	3.340e-5	1.53	3.60

Table 5: Errors and convergence rates for the VG model for various values of N_τ.

Model	S				
	20	30	40	50	60
CGMY	0.37224	4.82891	13.7801	24.05797	34.54281
Meixner	0.23802	2.11077	12.51470	23.74673	33.78861
GH	0.29120	2.46570	11.84807	22.08239	32.32227

Table 6: The reference European option values under Lévy processes.

(**RMSRE**) as the size of grid points (N_x, N_τ) changes where

$$\textbf{RMSRE} = \sqrt{\frac{1}{5}\sum_{i=1}^{5}\left(\frac{\hat{\mathcal{C}}(S_i,T)-\mathcal{C}(S_i,T)}{\hat{\mathcal{C}}(S_i,T)}\right)^2}, \tag{75}$$

such that $\hat{\mathcal{C}}$ represents the reference value of the European option at $S = \{20, 30, 40, 50, 60\}$ calculated for a grid $(2048, 524288)$ and the option values are given in Table 6

75

Example 3. Here an European option is priced under the three Lévy process classes with parameters $T = 0.5$, $E = 30$, $r = 0.1$, $q = 0$, $\sigma = 0.25$, $\varepsilon = 0.35$,

Model	Parameters
CGMY	$C = 0.5$, $G = 25$, $M = 25$ and $Y = 1.2$.
Meixner	$A = 0.3462$, $a = -3.7566$ and $b = 7.8994$.
GH	$\alpha = 3.8$, $\beta = -2.5$, $\delta = 0.2375$ and $\lambda = 2.755$

Table 7: The parameters for Lévy models used in Example 3.

	Model	CGMY			Meixner			**GH**		
	(N_x, N_τ)	**RMSRE**	Ratio	CPU (sec)	**RMSRE**	Ratio	CPU (sec)	**RMSRE**	Ratio	CPU (sec)
Scheme 1	(32,350)	3.633e-3	–	0.78	5.839e-4	–	0.57	7.013e-3	–	0.74
	(64,500)	1.392e-3	2.61	1.93	3.702e-4	1.58	1.43	1.964e-3	3.57	1.92
	(128,2.5e3)	2.545e-4	5.47	18.70	8.481e-5	4.36	13.64	4.699e-4	4.18	14.65
	(256,6e3)	8.079e-5	3.15	89.47	3.215e-5	2.64	65.10	1.227e-4	3.83	55.38
Scheme 2	(32,32)	2.116e-3	–	0.81	8.940e-4	–	0.47	6.910e-4	–	0.92
	(64,64)	8.932e-4	2.37	1.63	7.019e-4	1.27	0.86	6.008e-4	1.15	1.72
	(128,128)	2.617e-4	3.41	3.55	1.991e-4	3.52	2.38	1.727e-4	3.48	3.76
	(256,256)	5.536e-5	4.73	8.79	3.487e-5	5.71	3.87	6.718e-5	2.57	5.81

Table 8: Comparison of Scheme errors and CPU times for European option

$M = 15$, $x_{\min} = 0$, $x_{\max} = 90$ and the other parameters for Lévy models are listed in Table 7. The variation of the **RMSRE** for several grids are given in Table 8, the ratio and the computational time for schemes 1 and 2.

Example 4. This example related to stability of scheme 1 is performed to plot the amplification factor G given by (31) for European options under Lévy models with the parameters given in Example 3 for $N_x = 256$ and $N_\tau = 6e3$ as shown in Fig 2 for $\theta \in [0, 2\pi]$. Also, the dependence of the local truncated error of the integral part given by (52) on the degree of Laguerre polynomial M is reported for several values of $\hat{\xi}$ in Table 9.

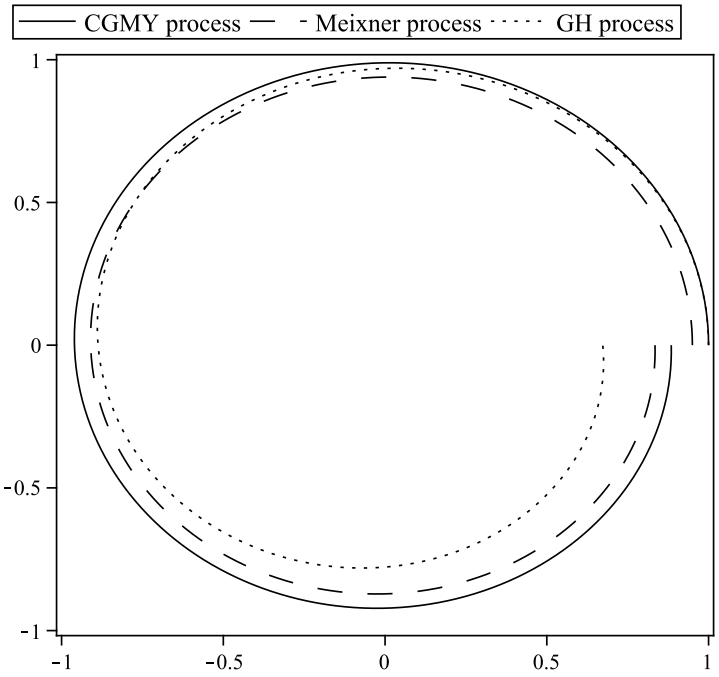

Fig. 2. The amplification factor G under stability condition.

Example 5. Here, we deal with the LCP for American option under CGMY, Meixner and **GH** process with parameters as in Example 3 while $q = 0.05$ solved numerically using the scheme (67)-(70). Associated **RMSRE** is given in Table 10. The PSOR and MG are implemented to obtain numerical approximations, the comparison based on the accuracy and elapsed time are presented in Table 10. The reference values obtained for a grid $(2048, 524288)$ are listed in Table 11.

The following example study the behavior of the option under CGMY process for Barrier call up-out case. First, this model is constituted by (13) with the following boundary and initial conditions

$$\begin{aligned} V(x_0,\tau) &= 0, \quad x_0 = \exp[(r-q-\gamma(\varepsilon))\tau]L, \\ V(x_f,\tau) &= 0, \quad x_f = \exp[(r-q-\gamma(\varepsilon))\tau]U, \end{aligned} \tag{76}$$

$$V(x,0) = \max(x-E,0), \quad x < x_f, \tag{77}$$

		Errors		
M	$\hat{\xi}$	CGMY	Meixner	**GH** process
10	12.66	9.911e-5	1.026e-4	1.861e-6
	30.94	1.904e-4	5.752e-6	1.472e-5
	42.18	2.949e-5	3.733e-6	9.991e-6
20	12.66	1.391e-8	-5.649e-8	6.647e-9
	30.94	2.044e-11	7.172e-10	2.1726e-10
	42.18	-1.347e-11	-4.592e-10	-1.4934e-12
30	12.66	4.743e-15	-1.029e-14	1.168e-14
	30.94	-2.468e-17	1.163e-14	1.996e-18
	42.18	-1.819e-17	8.673e-15	1.475e-18

Table 9: The Truncated error for the integral part

	Model	CGMY			Meixner			**GH**		
	(N_x, N_τ)	**RMSRE**	Ratio	CPU (sec)	**RMSRE**	Ratio	CPU (sec)	**RMSRE**	Ratio	CPU (sec)
PSOR	(32,32)	2.362e-2	–	0.35	1.685e-2	–	0.19	3.548e-2	–	0.23
	(64,64)	6.775e-3	3.49	1.44	7.492e-3	4.91	0.95	9.832e-3	3.74	1.02
	(128,128)	1.403e-3	4.83	4.36	2.099e-3	3.57	3.84	1.860e-3	5.28	4.15
	(256,256)	3.727e-4	3.76	9.45	7.374e-4	2.85	8.74	8.112e-4	2.59	9.38
MG	(32,32)	1.527e-2	–	0.32	1.248e-2	–	0.19	2.394e-2	–	0.22
	(64,64)	4.421e-3	3.45	1.12	4.395e-3	2.83	0.72	9.643e-3	2.49	0.95
	(128,128)	8.0987e-4	5.46	2.13	8.052e-4	4.97	1.23	2.175e-3	4.43	2.96
	(256,256)	2.1532e-4	3.76	3.28	2.729e-4	3.24	2.93	6.173e-4	3.52	3.86

Table 10: The **RMSRE** for American option under Lévy processes

Model	S				
	20	30	40	50	60
CGMY	0.84963	6.74776	12.17171	22.94875	32.75316
Meixner	0.56471	4.35491	11.54473	21.24781	31.83748
GH	0.53621	5.17148	11.01960	20.75684	31.64827

Table 11: The reference American option values.

where L and U are the lower and upper boundaries for the underlying asset S. Consequently, the corresponding finite difference scheme is given by (24) with

$$V_0^n = 0, \quad V_f^n = 0, \quad 0 \leq n \leq N_\tau - 1, \tag{78}$$

$$V_j^0 = \max(x_j - E, 0), \quad 0 \leq x_j \leq x_f. \tag{79}$$

Example 7. Here, we have an option with parameters $T = 1$, $E = 100$, $r = 0.05$, $q = 0$, $\sigma = 0.15$, $M = 15$, $x_{\min} = 0$, $x_{\max} = 125$ under Variance Gamma with parameters $\mathcal{G} = 14.4$, $\mathcal{M} = 60.2$, $C = 0.5$ and $U = 120$, the parameters are selected as in [17]. Table 12 reveals the absolute error at $S = 100$ for several values of N_x while $N_\tau = 4e3$, also obtained for different values of N_τ while $N_x = 128$ and the associated convergence rates. On the other hand, the numerical experiment has been done for the option under CGMY process for pure jump case with the following parameters $C = 4$, $\mathcal{G} = 50$, $\mathcal{M} = 60$, $Y = 0.7$, $r = 0.05$, $q = 0.02$, $M = 15$ as in [41]. The associated absolute error and its convergence ratio are presented in Table 13 for various values of N_x and N_τ.

Acknowledgements

This work has been partially supported by the European Union in the FP7-PEOPLE-2012-ITN program under Grant Agreement Number 304617 (FP7

N_x	**AE**	α	N_τ	**AE**	β
32	4.728e-3	–	5e2	3.854e-3	–
64	1.377e-3	1.78	1e3	1.857e-3	1.05
128	3.819e-4	1.85	2e3	9.779e-4	0.93
256	9.816e-5	1.96	4e3	4.945e-4	0.98

Table 12: The variation of the error for several values of N_x and N_τ. when $\sigma = 0.15$

(N_x, N_τ)	**AE**	Ratio
(32,350)	3.907e-3	–
(64,500)	1.607e-3	2.43
(128,5e3)	3.265e-4	4.92
(256,6e3)	8.392e-5	3.89

Table 13: The associated error for various grids for pure jump case.

Marie Curie Action, Project Multi-ITN STRIKE-Novel Methods in Computational Finance) and the Ministerio de Economía y Competitividad Spanish grant MTM2013-41765-P.

References

[1] F. Black, M. Scholes, The pricing of options and corporate liabilities, J. Political Economy, 81 (1973) 637–654.

[2] S. L. Heston, A closed-form solution for options with stochastic volatility with applications to bond and currency options, The Review of Financial Studies, 6 (1993) 327–343.

[3] J. C. Cox and S. A. Ross, The valuation of options for alternative stochastic processes, J. Financial Economics, 3 (1976) 145–166.

[4] R. C. Merton, Option pricing when the underlying stocks are discontinuous, J. Financ. Econ., 5 (1976) 125–144.

[5] L. Andersen,J. Andreasen, Jump-diffusion processes: Volatility smile fitting and numerical methods for option pricing, Rev. of Deriv. Res., 4 (2000), 231–262.

[6] S. G. Kou, A jump diffusion model for option pricing, Management Science, 48 (2002) 1086–1101.

[7] J. Toivanen, Numerical valuation of European and American options under KOU's jump-diffusion model, SIAM J. SCI. COMPUT, 30(4) (2008) 1949–1970.

[8] P. Carr, H. Geman, D. B. Madan, and M.Yor, The fine structure of asset returns: an empirical investigation, Journal of Business, 75(2) (2002) 305–332.

[9] S. I. Boyarchenko, S. Z. Levendorskii, Option pricing for truncated Levy processes, International Journal of Theoretical and Applied Finance, 3(3) (2000) 549-552.

[10] W. Schoutens, J.L. Teugels, Lévy processes, polynomials and martingales, Cummun. Statist.-Stochastic Models, 14(1 and 2) (1998) 335-349.

[11] D. Madan, M. Yor, Representing the CGMY and Meixner Lévy processes as time changed Brownian motions, Journal of Computational Finance, 12(1) (2008) 27-47.

[12] W. Schoutens, *Lévy processes in finance: pricing financial derivatives*, Wiley: New York, 2003.

[13] O. E. Barndorff-Nielsen, Exponentially decreasing distributions for the logarithm of particle size, Proceeding of the Royal Society of London, A353 (1977) 401–419.

[14] E. Eberlein, Application of generalized hyperbolic Lvy motions to finance, *Lévy Processes: Theory and Applications, O.E. Barndorff-Nielsen, T. Mikosch, and S. Resnick (eds.)*, Springer, (2001) 319–337

[15] Eberlein, E., Keller, U., and Prause, K., New insights into smile, mispricing and Value at Risk: The hyperbolic model, Journal of Business, 71 (1998) 371–405.

[16] R. Cont, P. Tankov, *Financial modeling with jump processes*, Chapman & Hall/CRC financial mathematics series, 2004.

[17] R. Cont, E. Voltchkova, A finite difference scheme for option pricing in jump diffusion and exponential Lévy models, SIAM Journal on Numerical Analysis, 43(4) (2005) 1596–1626.

[18] I. R. Wang, J. W. Wan, P. A. Forsyth, Robust Numerical Valuation of European and American Options under the CGMY process. J. Comput. Finance (2007) 10, 31–69.

[19] N. Rambeerich, D. Y. Tangman, M. Bhuruth, Numerical pricing of American options under infinite activity Lévy processes. The Journal of Futures Markets (2011) 31, 809–829.

[20] R. Company, L. Jódar, M. Fakharany, Positive solutions of European option pricing with CGMY process models using double discretization difference schemes, Abstr. Appl. Anal. 2013 (2013) 1-11.

[21] W. Schoutens, J. Cariboni, *Lévy process in credit risk*, John Wiley & Sons Ltd (2009).

[22] M. Abramowitz, I. A. Stegun, *Handbook of mathematical functions: with formulas, graphs, and mathematical tables*, Dover Books on Mathematics, (1961).

[23] P. J. Davis, P. Rabinowitz, *Methods of numerical integration*, Second Edition, Academic Press, New York, USA, 1984.

[24] R. Kangro, R. Nicolaides, Far field boundary conditions for Black–Scholes equations, SIAM Journal on Numerical Analysis 38 (4) (2000) 1357–1368.

[25] J. C. Strikwerda, *Finite difference schemes and partial differential equations*, second ed., Siam, 2004.

[26] G. D. Smith, *Numerical solution of partial differential equations: finite difference methods* (3rd ed.), Clarendon Press, Oxford, UK, 1985.

[27] B. Düring, M. Fournié,High-order compact finite difference scheme for option pricing in stochastic volatility models, Journal of Computational and Applied Mathematics 236 (2012) 4462-4473.

[28] B. Gustafsson, H. O. Kreiss and J. Oliger, *Time dependent problems and difference methods*, John Wiley & Sons, Inc., 1995.

[29] A. Almendral, C. W. Oosterlee, On American options under the Variance Gamma process, Applied Mathematical Finance, 14 (2) (2007) 131-152.

[30] P. Linz, *Analytic and numerical methods for Volterra equations*, SIAM, Philadelphia, USA, 1985.

[31] F. B. Hildebrand, *Introduction to numerical analysis, second edition*, Dover Publications, INC. Mineola, New York, 1987.

[32] S. Ikonen, J. Toivanen, Efficient numerical methods for pricing American options under stochastic volatility, Wiley J. Numerical methods for partial differential equations, 24(1) (2008) 104–126.

[33] S. Ikonen and J. Toivanen, Operator splitting methods for American option pricing, Appl. Math. Lett. 17 (2004) 809-814.

[34] C. W. Oosterlee, On multigrid for linear complementarity problems with application to American-style options, Electron. Trans. Numer. Anal., 15 (2003) 165–185.

[35] C. W. Cryer, The solution of a quadratic programming problem using systematic overrelaxation, SIAM J. Control, 9 (1971) 385–392.

[36] S. Ikonen, J. Toivanen, Operator splitting methods for pricing American options under stochastic volatility, Numer. Math. 113 (2009) 299-324.

[37] W. L. Briggs, V. E. Henson, S. F. McCormick, *A multigrid tutorial*, SIAM, Philadelphia, PA, second ed., 2000.

[38] P. Wesseling, *An introduction to multigrid methods*, John Wiley & Sons, 1992.

[39] W. Hackbusch, *Multi-grid methods and applications*, Springer, 1985.

[40] D. B. Madan, P. Carr, E. C. Chang, The Variance Gamma process and option pricing, European Finance Review, 2 (1998) 79–105.

[41] F. Fang, C. W. Oosterlee, Pricing early-exercise and discrete barrier options by Fourier-cosine series expansions, Numer. Math. 114 (2009) 27–62.